EELS modelling of graphitisation

C R Seabourne[1], R Brydson[1], A P Brown[1], C D Latham[2], M I Heggie[2] and A J Scott[1]

[1]Institute for Materials Research, SPEME, Faculty of Engineering, University of Leeds, Leeds, LS2 9JT, UK
[2]Department of Chemistry, Faculty of Engineering and Physical Sciences, University of Surrey, Guildford, GU2 7XH, UK

E-mail: c.r.seabourne@leeds.ac.uk

Abstract. The impact of graphitisation-type processes on the carbon *K*-edge ELNES is explored for model systems using the CASTEP density functional theory code. For *c* lattice direction expansion, contraction of spectral peaks occurs between 20 and 27 eV above the edge onset, for *a/b* lattice dimension expansion spectral peaks are heavily compressed in terms of energy separation and are shifted towards the edge-onset, consistent with a $1/a^2$ relationship. For a nanotube model system, it is shown that for higher curvature, an additional feature was observed in the spectrum ~5 eV, arguably consistent with 'fullerene'-type character.

1. Introduction

Graphitic materials are now amongst the most characterized and written about systems in science, and the range of systems is considerable; nanotubes [1], fullerenes [2,3], potentially tunable cone-type structures [4,5], the wonder-material graphene and doped derivatives [6-10], and further discoveries regarding the folding and other unusual behaviours of the material [11]. Graphene is ideal for study in the electron microscope due to its inherent thinness, avoiding effects such as dechanneling in atomic columns in the specimen [12], though careful microscope parameters must be chosen so as to avoid knock-on damage [13]. A similar approach can be adopted when studying bulk graphite in the microscope, to obtain high resolution information. This high level information can include the electron energy-loss spectrum (EELS) of graphite. This work focuses on the core-loss region (carbon *K* edge), in particular using density functional theory (DFT) modelling, but one of the authors of this paper has also considered multiple scattering (MS) as a technique to model the edge [14].

DFT modelling is used to address two particular challenges regarding the carbon *K*-edge energy-loss near edge structure (ELNES) and the potential impacts of graphitisation, amorphisation and irradiation damage in nuclear reactors or the electron microscope; lattice expansion/contraction in the *a/b* and *c* directions, and the influence of curvature on the *K*-edge ELNES, as considered by using a series of nanotube examples. This work should allow us to relate experimentally observed changes in the carbon *K*-edge ELNES (upon for example irradiation or heating) to structural changes as modelled by the systems in this work. This may be particularly helpful if it is difficult to measure lattice parameters or curvature of nanoscale carbons experimentally.


Content from this work may be used under the terms of the Creative Commons Attribution 3.0 licence. Any further distribution of this work must maintain attribution to the author(s) and the title of the work, journal citation and DOI.
Published under licence by IOP Publishing Ltd

2. Density functional theory methodology

For all experiments, the CASTEP DFT code was used for ELNES predictions [15,16]. It is important when using a DFT code to properly converge relevant parameters to ensure accurate results. This was carried out by converging parameters directly against the ELNES results themselves, thus following a methodology previously outlined in the literature [17]. In this instance, the key parameters for convergence are the basis-set size, as defined by the kinetic energy cut-off value, and the density of *k*-point sampling in reciprocal space, in these cases using a Monkhorst-Pack type grid [18].

A bulk graphite crystal was chosen as the convergence system. For the kinetic energy cut-off, an initial value of 400 eV was chosen, and upon doubling that value to 800 eV, there was virtually no change in the predicted, unbroadened ELNES result (the carbon *K* edge for a single atom in the standard unit cell), thus this parameter was considered to be converged. A similar process was carried out for the *k*-points grid, which was doubled from 12×12×4 to 24×24×8. In this case, barely any changes were observable by visual inspection to the predicted spectra, but a further mathematical analysis was carried out. For a range of points from -2 eV to 50 eV, the modulus percentage change between the two results was found at each data point on the energy axis. This percentage change was then averaged across all the data points, and found to be less than 10 %, confirming only small changes occur, thus the parameter is converged.

Table 1: Summary of converged parameters for carbon *K* edge calculations, using the CASTEP DFT code. The *c* lattice parameter was subsequently optimised to a value closer to experiment.

Structural information of model convergence system	Kinetic energy cut-off / eV	Density of *k*-points in reciprocal space / $Å^{-1}$
$a = b = 2.46$ Å, $c = 6.80$ Å $\alpha = \beta = 90°$, $\gamma = 120°$	800	0.018

Where the predicted spectra were then subject to broadening, an energy-dependent final state lifetime based scheme was used, as presented previously [19].

Following initial convergence experiments, a Broyden, Fletcher, Goldfarb, Shanno (BFGS) geometry optimisation was carried out with a generalized gradient approximation Tkatchenko Scheffler (GGA-TS) correction [20], leading to optimised cell dimensions of; $a=b = 2.454$ Å, $c = 6.673$ Å.

3. Results

3.1. Expansion / contraction of lattice c dimension

From a geometry optimised starting point of $c = 6.673$ Å, with the $a=b$ lattice parameter fixed at 2.454 Å, the *c* dimension was varied by ± 10 % and ± 5 %. This led to a total of five predicted carbon *K* edge spectra, for expansion / contraction of the *c* dimension, Figure 1. Contraction physically speaking might represent behaviour under pressure; expansion is a simplified approach to understand trends in for example the intercalation of cations between graphite layers (although we do not seek to account for the resultant change in chemistry). Calculations were carried out in the ground electronic state. In each case, there were two inequivalent atoms in the unit cell, whose spectra are simply averaged. It is assumed their chemical environments are sufficiently similar so as to make adjusting for an absolute energy-onset difference not relevant.

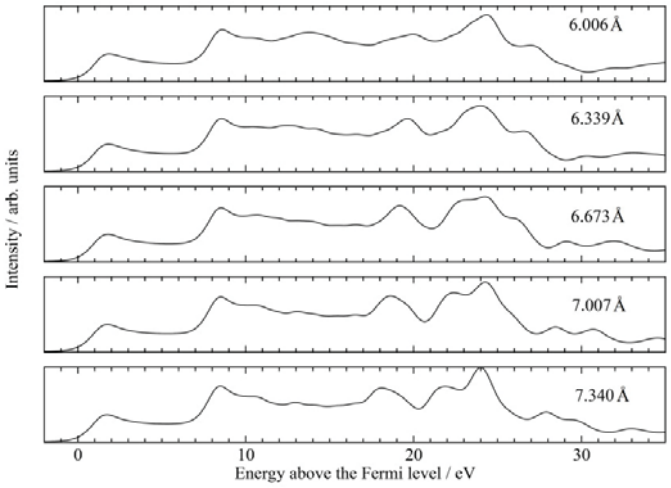

Figure 1. Predicted carbon *K*-edge ELNES for graphite using the CASTEP DFT code, carried out in the ground electronic state. The *c* axis lattice parameters are labelled in each case, for constant *a*=*b*. The results are shown with a 0.4 eV Gaussian broadening.

We observe contraction of peaks between 20 and 27 eV (above the edge onset) as the *c* axis parameter increases (spectral peaks move closer together), and arguably some loss in intensity between 13-16 eV. Also a significant peak develops for smaller *c* values at ~27 eV.

3.2 Expansion / contraction of a/b lattice parameters

As in section 3.1, the *a/b* lattice parameter was varied from 2.454 Å by ± 5 % and ± 10 %, with the *c* lattice parameter kept constant, Figure 2. Contracted cells are obviously under considerable strain considering the standard C-C bond distance of 1.42 Å.

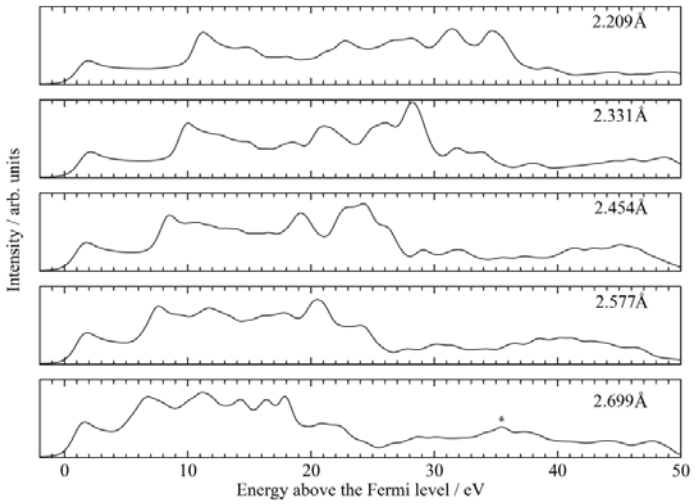

Figure 2. Predicted carbon K-edge ELNES for graphite, using the CASTEP DFT code, carried out in the ground electronic state. The *a/b* lattice parameters are labelled in each case, for constant *c*. The results are shown with a 0.4 eV Gaussian broadening.

Based on previous work, various peak separations vary as a function of $1/a^2$ [21,22]. Plotting the separation in energy between the first two peaks versus $1/a^2$ leads to a linear fit, with a R^2 regression coefficient of 0.995, similarly the energy separation from the π* peak (the first in the spectrum) to the peak labelled with an asterisk (or its equivalents for the different lattice parameter values) plotted versus $1/a^2$ is also a linear fit, regression coefficient of 0.98, and there are other similar examples.

3.3 Nanotube radius of curvature

Single-wall nanotubes were constructed as $n \times m$ ($n=m$ armchair, diameter = $0.783(n^2 + nm + m^2)^{1/2}$ Å). The C-C bond length was 1.42 Å. Inequivalent positions gave similar spectra.

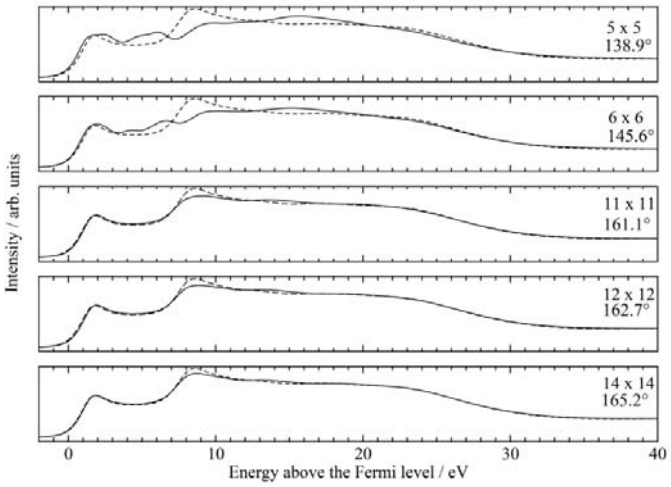

Figure 3. Predicted carbon K-edge ELNES for various labelled nanotube sizes (also labelled are angles between adjacent hexagons, which for graphene is 180°), using the CASTEP DFT code, carried out in the ground electronic state, with inequivalent positions not averaged due to similarity. The results are shown with the addition of energy-dependent final state lifetime broadening [19]. Shown on each plot is a dashed line, which is a predicted spectrum for bulk graphene (with a 25 Å vacuum to simulate the monolayer).

For increasing nanotube radius of curvature the spectrum begins to approach that of graphene [23]. When the system is however 'more curved', for example for the 5×5 nanotube (diameter 6.78 Å), an additional peak is observed at ~5 eV above the edge onset – this may be something that is indicative in experimental spectra, indicating curvature in a specimen, or perhaps fullerene character [24].

4. Conclusions

Modelled carbon *K*-edge ELNES show that curvature may lead to an additional feature at ~5 eV above the edge onset and that for *a/b* lattice expansion peaks are compressed closer together towards the Fermi level. These are structural trends useful when analysing carbon *K*-edge ELNES from irradiated samples for example, where it is not necessarily trivial to measure lattice parameters or 'curvature'. Future work may consider multi-walled nanotubes and displacement from AB graphite stacking.

5. References

[1] Iijima S and Ichihashi T 1993 *Nature* 363, 603
[2] Kroto H W et al. 1985 *Nature* 318, 162
[3] Howard J B et al. 1992 *Carbon* 30, 1183
[4] Krishnan A et al. 1997 *Nature* 388, 451
[5] Hage F S et al. 2013 *Nanoscale*, submitted
[6] Novoselov K S et al. 2004 *Science* 306, 666
[7] Novoselov K S et al. 2005 *Proc. Natl Acad. Sci. USA* 102, 10451
[8] Geim A K and Novoselov K S 2007 *Nat. Mater.* 6, 183
[9] Geim A K 2009 *Science* 19, 1530
[10] Ramasse Q M et al. 2013 *Nano Lett.* ASAP, dx.doi.org/10.1021/nl304187e
[11] Heggie M I et al. 2011 *J. Nucl. Mater.* 413, 150
[12] Egerton R F 2009 *Rep. Prog. Phys.* 72, 016502
[13] Gass M H et al. 2008 *Nat. Nanotech.* 3, 676
[14] McCulloch D G and Brydson R 1996 *J. Phys.: Condens. Matter* 8, 3835
[15] Clark S J et al. 2005 *Z. Kristallogr.* 220, 567
[16] Gao S P et al. 2008 *Phys. Rev. B* 77, 115122
[17] Seabourne C R et al. 2009 *Ultramic.* 109, 1374
[18] Monkhorst H J and Pack J D 1976 *Phys. Rev. B* 13, 5188
[19] Moreau P et al. 2006 *Phys. Rev. B* 73, 195111
[20] Tkatchenko A and Scheffler M 2009 *Phys. Rev. Lett.* 102, 073005
[21] Daniels H et al. 2007 *Phil. Mag.* 87, 4073
[22] Craven A J 1995 *J. Micros.* 180, 250
[23] Suenaga K and Koshino M 2010 *Nature* 468, 1088
[24] Zhang Z et al. 2011 *Carbon* 49, 5049